



Investigations on the effects of multi-layered coated inserts in machining Ti–6Al–4V alloy with experiments and finite element simulations

T. Özel (2)^{a,*}, M. Sima^a, A.K. Srivastava (3)^b, B. Kaftanoglu (1)^c

^a Manufacturing Automation Research Laboratory, Department of Industrial and Systems Engineering, Rutgers University, NJ, USA

^b TechSolve Inc., Cincinnati, OH, USA

^c Department of Manufacturing Engineering, Atılım University, Ankara, Turkey

ARTICLE INFO

Keywords:
Machining
Finite element method
Titanium
Tool

ABSTRACT

This paper presents investigations on turning Ti–6Al–4V alloy with multi-layer coated inserts. Turning of Ti–6Al–4V using uncoated, TiAlN coated, and TiAlN + cBN coated single and multi-layer coated tungsten carbide inserts is conducted, forces and tool wear are measured. 3D finite element modelling is utilized to predict chip formation, forces, temperatures and tool wear on these inserts. Modified material models with strain softening effect are developed to simulate chip formation with finite element analysis and investigate temperature fields for coated inserts. Predicted forces and tool wear contours are compared with experiments. The temperature distributions and tool wear contours demonstrate some advantages of coated insert designs.

© 2010 CIRP.

1. Introduction

Titanium alloys such as Ti–6Al–4V offer high strength-to-weight ratio, high toughness, superb corrosion resistance, and biocompatibility and are increasingly used in aerospace and biomedical applications. However, titanium alloys are difficult to machine due to their low thermal conductivity and diffusivity, high rigidity and low elasticity modulus and high chemical reactivity at elevated temperatures [1]. These alloys exhibit serrated and cyclical chip formation resulting in detrimental tool vibrations [2]. Titanium alloy machining performance can be increased by improving cutting tool materials and coatings [3,4]. Cubic boron nitride (cBN) material offers outstanding properties such as high hardness and wear resistance. However, cBN material has lower toughness and is not suitable for forming inserts into complex shapes. Recently, cBN coatings have been explored by applying several deposition techniques. Among these, physical vapor deposition (PVD) has been preferred since thinner coatings can be deposited and sharp edges and complex shapes can be easily coated at lower temperatures. On the other hand, coating applied affects the edge radius of the inserts and must be taken into consideration during tool performance analysis [4].

In this research, single and multi-layer TiAlN and cBN coatings are experimented on tungsten carbide inserts (WC/Co) for possible improvements in machining of Ti–6Al–4V alloy. Positive tool geometry WC/Co inserts are coated by cBN using a PVD system. Machining performance of multi-layered coated inserts is examined in longitudinal turning of titanium alloy (Ti–6Al–4V) without using coolant. The performance of uncoated, TiAlN coated, cBN

coated and multi-layer cBN + TiAlN coated tungsten carbide inserts is compared in terms of cutting forces and tool wear.

In addition, finite element (FE) simulations are utilized in investigating the tool temperatures and wear development. Two dimensional and three dimensional FE simulations have been designed and conducted to predict forces, temperatures and tool wear to investigate the advantages of coatings in machining of Ti–6Al–4V. Finite element modelling and simulations of chip formation process in titanium alloy machining present significant challenges due to the nature of complicated dynamic material behaviour of these alloys at elevated temperatures, strain and strain rates. In general, adiabatic shearing is considered as responsible for serrated chip formation. Increasing temperatures in the primary shear zone due to shear deformation weaken the material by thermal softening; therefore, the deformation is concentrated in shear bands, leading to serrated chip formation [5]. Although it is also possible to simulate serrated chip formation by using damage models [6], in this paper it is assumed that serration is caused by adiabatic shearing.

2. Material constitutive model for Ti–6Al–4V and validation

In FE models, a constitutive material model is required to relate the flow stress to strain, strain rate and temperature, which often obtained from Split-Hopkinson pressure bar (SHPB) tests performed under various strain rates and temperatures. Dynamic material behaviour for Ti–6Al–4V titanium alloy has been widely published in literature [7,8]. Nemat-Nasser [7] reported that a phenomenon known as strain (flow) softening is observed which is responsible for adiabatic shearing in titanium alloys. Localized softening is described as offering less resistance to local deformations due to rearrangement of dislocations caused by subsequent cycling in hard materials. This phenomenon is usually seen during

* Corresponding author.

an increase in strain beyond a critical strain value. Specifically, Lee and Lin [8] investigated temperature and strain-rate sensitivity of Ti–6Al–4V and presented flow stress data at temperatures from 20 to 1100 °C and strain rates ranging from 800 up to 3300 s⁻¹. They used The Johnson–Cook (JC) material model to represent their flow stress data. However, their model did not include temperature-dependent strain softening effect.

2.1. Modified material model

A modification to the JC model is offered to include strain (flow) softening effects at elevated temperatures as proposed by Calamaz et al. [9]. In this study, further modifications to the strain hardening part of the JC model by including strain softening at higher strain values and thermal softening part are proposed and the model is given in Eq. (1). In this model, the influence of strain, strain rate, temperature and temperature-dependent strain softening on the flow stress is defined by four multiplicative terms.

$$\sigma = \left[A + B\varepsilon^n \left(\frac{1}{\exp(\varepsilon^a)} \right) \right] \left[1 + C \ln \frac{\dot{\varepsilon}}{\dot{\varepsilon}_0} \right] \left[1 - \left(\frac{T - T_0}{T_m - T_0} \right)^m \right] \left[D + (1 - D) \left[\tan h \left(\frac{1}{(\varepsilon + p)^r} \right)^s \right] \right] \quad (1)$$

where $D = 1 - (T/T_m)^d$, $p = (T/T_m)^b$, σ is flow stress, ε is true strain, $\dot{\varepsilon}$ is true strain rate, $\dot{\varepsilon}_0$ is reference true strain, and T , T_m , T_0 are work, material melting and ambient temperatures respectively.

The experimental flow stress data by Lee and Lin [8] has been taken as the base for this modified material model. The most optimum set of model parameters that was identified with inverse analysis are; $A = 782.7$ MPa, $B = 498.4$ MPa, $n = 0.28$, $C = 0.028$, $m = 1.0$, $a = 2$, $s = 0.05$, $r = 2$, $d = 1$, $b = 5$. The details of this methodology are outlined in the work by Özel et al. [10].

2.2. Orthogonal cutting tests

Orthogonal turning of Ti–6Al–4V titanium alloy tubes (50.8 mm in diameter and 3.175 mm in thickness) have been performed using uncoated and TiAlN coated tungsten carbide (WC/Co) cutting tools in a rigid CNC turning centre at TechSolve Inc. The cutting forces were measured with a force dynamometer and high-speed data acquisition devices. The experiments have been conducted using tool holders with 0° and 5° rake angle (γ) at a cutting speed of $v_c = 120$ m/min and three different feeds ($f = 0.075, 0.1, 0.125$ mm/rev). Images of micro-chip geometries were captured with optical digital microscopy.

2.3. 2D finite element simulations and validation

Finite element model is developed using updated Lagrangian (DEFORM-2D) software in which chip separation from workpiece is achieved with continuous remeshing. A plane-strain coupled thermo-mechanical analysis was performed. In these simulations, serrated chip formation process is simulated from the incipient to the steady-state by using adiabatic shearing based on strain (flow) softening elasto-viscoplastic work material assumption. The

Table 1
Mechanical and thermo-physical properties of work and tool materials and friction values used in FE simulations.

	Ti–6Al–4V	WC/Co	(Ti,Al)N	cBN
$E(T)$ [MPa]	$0.7412^*T + 113375$	$5.6e^5$	$6.0e^5$	$6.52e^5$
$\alpha(T)$ [mm mm ⁻¹ °C ⁻¹]	$3.10^{-9}*T + 7.10^{-6}$	$4.7e^{-6}$	$9.4e^{-6}$	$5.2e^{-6}$
$\lambda(T)$ [W m ⁻¹ °C ⁻¹]	$7.039e^{0.0011^*T}$	55	$0.0081^*T + 11.95$	100
$c_p(T)$ [N mm ⁻² °C ⁻¹]	$2.24e^{0.0007^*T}$	$0.0005^*T + 2.07$	$0.0003^*T + 0.57$	3.26

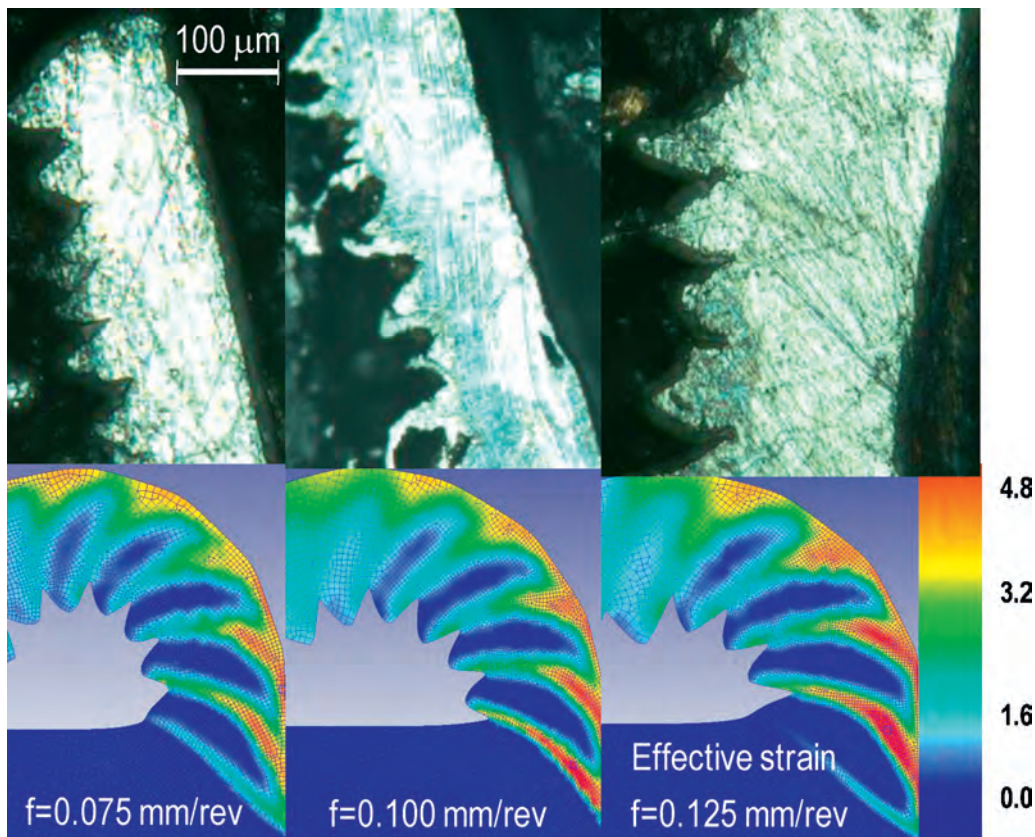


Fig. 1. Comparison of measured and simulated serrated chip geometry.

Table 2

Comparison of measured and simulated chip geometry.

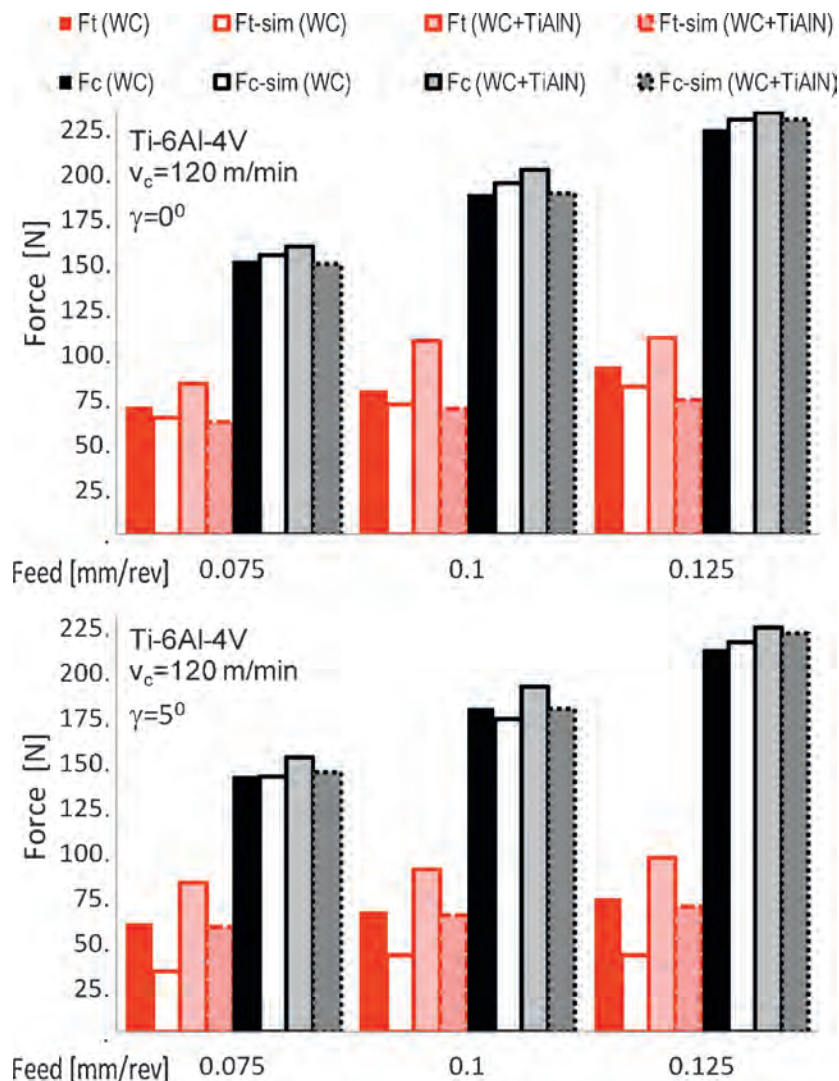
Cutting condition			Experimental		Simulated	
Tool	γ [°]	f [mm/rev]	h_1 [mm]	h_2 [mm]	h_1 [mm]	h_2 [mm]
WC/Co	0	0.075	0.095	0.133	0.081	0.101
WC/Co	0	0.1	0.130	0.192	0.108	0.135
WC/Co	0	0.125	0.104	0.177	0.120	0.163
WC/Co	5	0.125	0.156	0.230	0.135	0.171
WC/Co+TiAlN	0	0.1	0.137	0.182	0.107	0.135
WC/Co+TiAlN	0	0.125	0.140	0.216	0.133	0.172
WC/Co+TiAlN	5	0.1	0.102	0.158	0.107	0.134
WC/Co+TiAlN	5	0.125	0.120	0.208	0.135	0.172

simulations included a workpiece as elasto-viscoplastic with a mesh containing 10,000 quadrilateral elements. Tool is modelled as rigid with a mesh containing 2500 elements. Rake angles of 0° and 5° are employed in the tool geometry. Tool edge radius was estimated to be $r_\beta = 5 \mu\text{m}$ for uncoated WC/Co, and $r_\beta = 10 \mu\text{m}$ for TiAlN coated WC/Co respectively. Thermal boundary conditions are defined accordingly in order to allow heat transfer from workpiece to the cutting tool. The heat conduction coefficient (h) is taken as $1.0e^5 \text{ kW m}^{-2} \text{ K}^{-1}$ to allow rapid temperature rise in the tool. Mechanical and thermo-physical properties of titanium Ti-6Al-4V alloy are defined as temperature (T) dependent. Temperature-dependent (T in $^\circ\text{C}$) modulus of elasticity (E), thermal expansion (α), thermal conductivity (λ), and heat capacity (c_p) are given in Table 1.

In this paper, three contact regions are considered at the tool-chip interface: (i) a sticking region from the tool tip point to the end of the round edge curvature ($\tau = k$ where τ is frictional shear stress and k is the work material shear flow stress), (ii) a shear friction region ($m = \tau/k$) from the end of the curvature to the uncut chip thickness boundary ($m = 0.9$ for WC/Co, $m = 0.85$ for TiAlN), (iii) a sliding region along the rest of the rake face ($\mu = 0.7$ for WC/Co, $\mu = 0.5$ for TiAlN as the friction coefficient).

Simulations are run for 0.1 s cutting time. Comparison of simulated chips with experiments that are shown in Fig. 1 and Table 2 indicate close agreements. In Table 2, h_1 and h_2 indicate minimum and maximum serrated chip thickness respectively.

Predicted forces from simulations are compared with measured forces in orthogonal cutting tests of Ti-6Al-4V alloy tubes as

**Fig. 2.** Comparison of measured and simulated forces in orthogonal cutting tests.

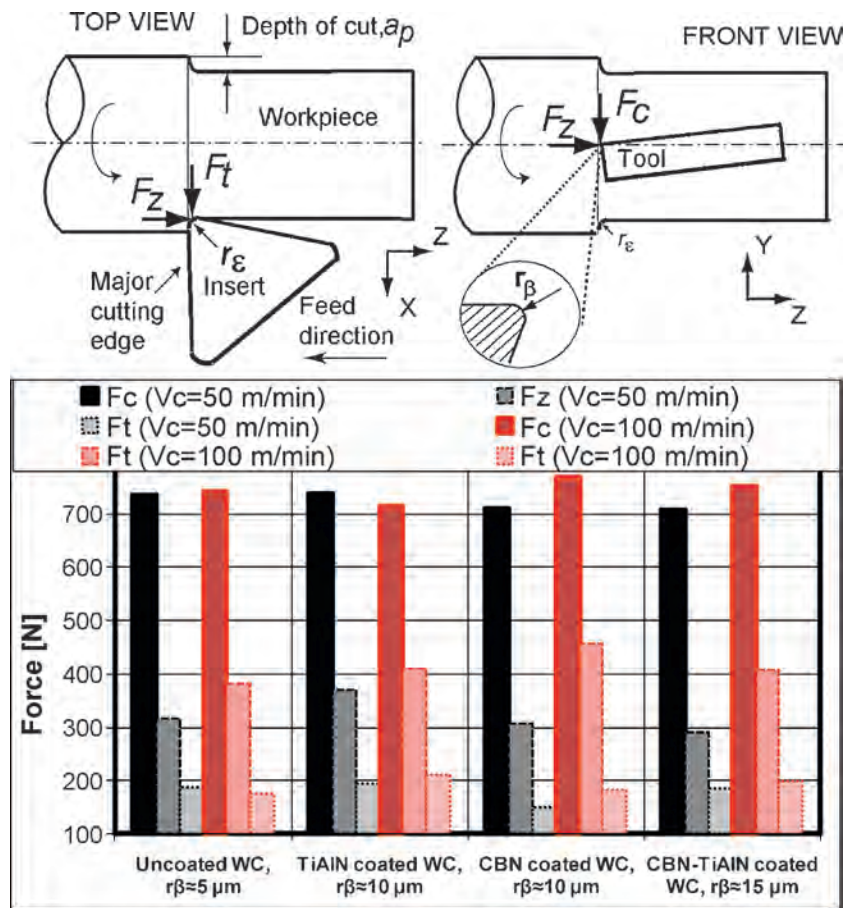


Fig. 3. Configuration of longitudinal bar turning experiments and force results.

shown in Fig. 2. Especially, cutting forces are in close agreements with 5% prediction error. Thrust force predictions which show 10–15% prediction error can be further improved with finer adjustments of friction regions and their values.

3. Experimental work

In this study, four different inserts at the same cutting conditions have been tested; uncoated/unalloyed tungsten carbide (WC/Co), tungsten carbide (WC/Co) PVD coated with TiAlN, tungsten carbide (WC/Co) PVD coated with cBN, tungsten carbide multi-layer PVD coated with cBN over TiAlN coating. Tungsten carbide (WC/Co) and PVD coated WC/Co with TiAlN inserts are coated with cBN by magnetron sputtering PVD system as mono

and multi-layer coatings at National Boron Research Institute (BOREN) in Turkey at a deposition pressure of 3×10^{-3} Torr and heater temperature of 100°C . Applied magnetron power is fixed at 900 W and argon to nitrogen gas ratio is adjusted to 5/1 and run at the lowest possible bias voltage to obtain uniform cBN coating.

Longitudinal turning of annealed Ti-6Al-4V titanium alloy bars (90 mm in diameter, 100 mm in length) was performed by using TPG432 type insert geometry (insert nose radius of $r_s = 0.8$ mm and relief angle of $\alpha = 11^\circ$) in a rigid CNC turning centre under dry machining conditions at Rutgers University Manufacturing Automation Research Laboratory. The inserts were used with a tool holder that provided 0° lead, -5° side rake, and -5° back rake angles. The cutting forces were measured with a force dynamometer mounted on the turret disk of the CNC turning centre. A

Table 3
Summary of FE simulation predictions.

Tool type	F_c [N]	F_t [N]	F_z [N]	T_{tool} [$^\circ\text{C}$]	T_{chip} [$^\circ\text{C}$]	dW/dt [mm/s]
WC/Co	590 (485–615)	93 (69–106)	229 (137–244)	785	791	0.0038
WC/Co + cBN	602 (490–612)	99 (86–100)	236 (145–280)	762	778	0.0019
WC/Co + TiAlN	571 (490–593)	98 (77–103)	228 (135–250)	811	810	0.0024
WC/Co + TiAlN + cBN	575 (481–606)	97 (81–115)	243 (166–286)	773	774	0.0025

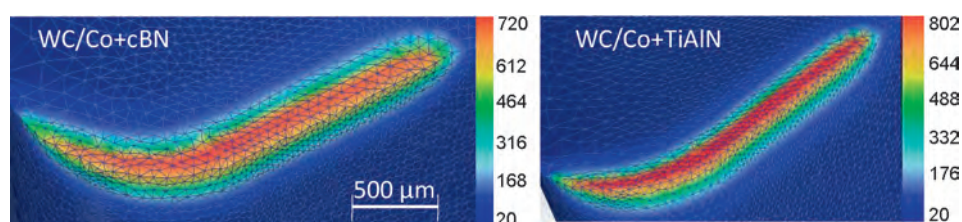


Fig. 4. Predicted temperature distributions in $^\circ\text{C}$.

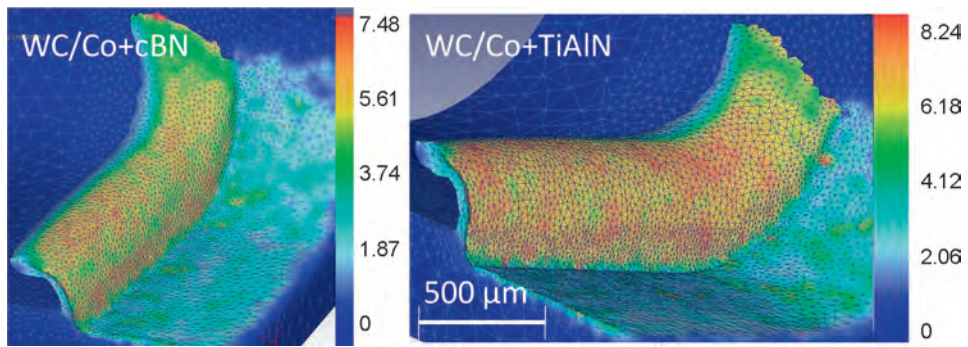


Fig. 5. Simulated chip formation with effective strain distributions.

constant depth of cut ($a_p = 2$ mm) and a constant feed ($f = 0.1$ mm/rev) were selected as cutting conditions. Each test was replicated at least twice. The averages of the measured forces for each insert are shown in Fig. 3.

In order to observe the performance of coatings at different cutting speeds, two sets of tests are done at cutting speeds of $v_c = 50$ and 100 m/min respectively. Thrust force was the lowest since inserts use 11° relief angle; hence flank contact area is very

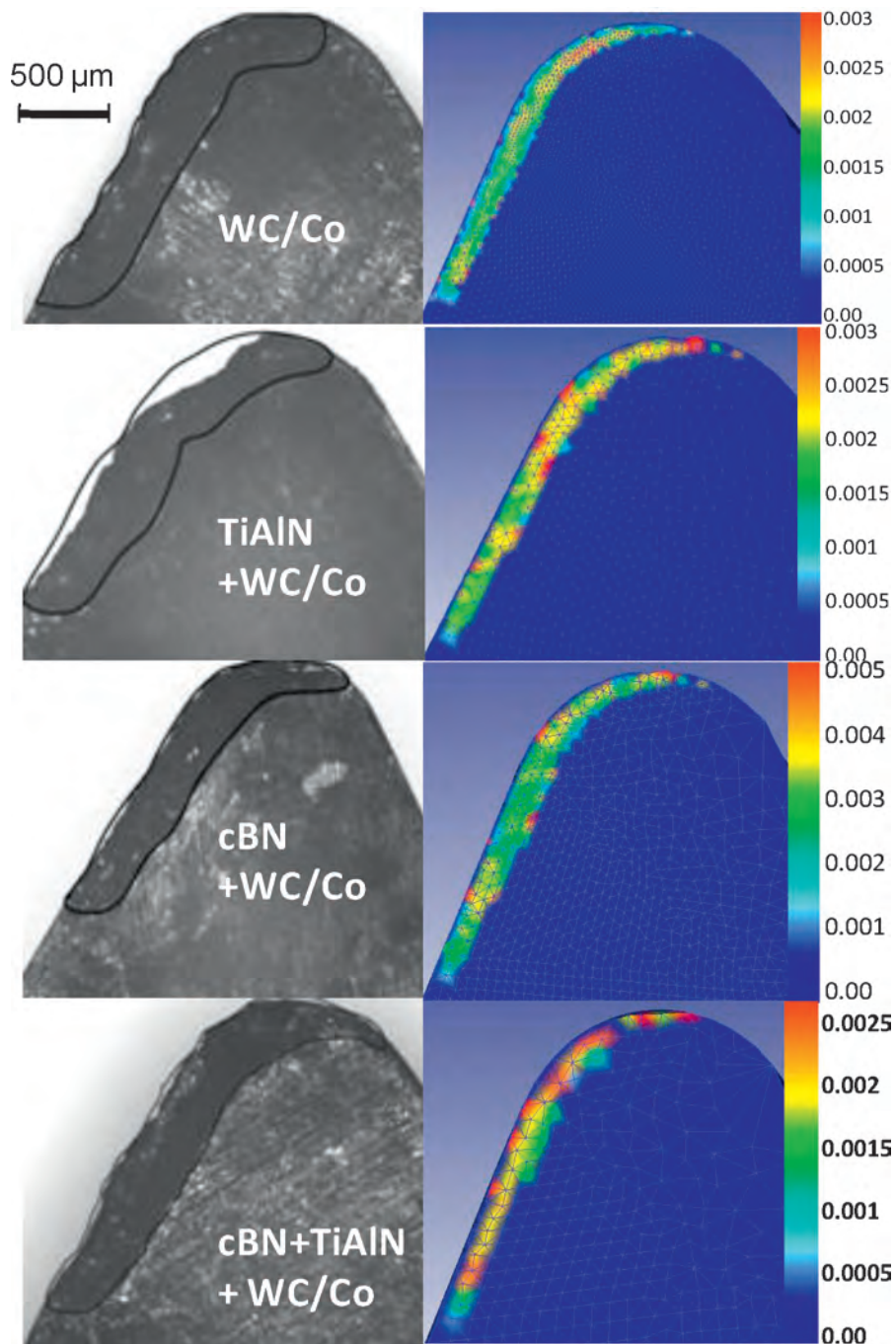


Fig. 6. Experimental and predicted wear rate distributions in [mm/s].

small. According to force measurements, cBN and cBN + TiAlN coated inserts exhibit lowest cutting forces at 50 m/min cutting speed but the highest at 100 m/min cutting speed. Moreover, the highest thrust force is seen in cBN coated WC/Co inserts at high cutting speed.

The advantage of cBN coatings on forces is apparent for the lower cutting speed. Adding cBN coating over TiAlN coating decreases forces. As cutting speed increases, the effect of larger edge radius (r_β) due to added layer of coatings (cBN and TiAlN) becomes the dominant mechanism on forces. This larger edge radius in multi-layer coated tools hinders the potential benefits of coatings, hence results in higher forces especially when cutting speed is doubled. Hence, it may be beneficial to modify edge preparation of the coated tools (TiAlN and cBN) to lower the cutting edge radius.

4. 3D finite element simulations

Several FE studies on 3D turning are presented in the past such as the work by Aurich and Bil [11] for segmented chip formation. In this study, updated Lagrangian FE modelling software (DEFORM-3D) was used. The workpiece is modelled as elastic-viscoplastic material where the material constitutive model of this deformable body is represented with modified J-C material model. The workpiece is represented by a curved model with 87 mm diameter which is consistent with the experimental conditions. Only a segment (3°) of the workpiece was modelled in order to keep the size of mesh elements small. Workpiece model includes 90,000 elements. The bottom surface of the workpiece is fixed in all directions. The cutting tool ($r_c = 0.8$ mm with 11° relief angle) is modelled as a rigid body which moves at the specified cutting speed by using 180,000 elements. A very fine mesh density is defined at the tip of the tool and at the cutting zone to obtain fine process output distributions. The minimum element size for the workpiece and tool mesh was set to 0.008 and 0.024 mm respectively. A tool edge radius of 5, 10 and 15 μm are designed for uncoated, single layer and multi-layer coated tools respectively for each simulation, since added layers in multi-coating design is increasing the edge radius of the inserts [4].

All simulations were run at the same experimental cutting condition ($v_c = 100$ m/min, $f = 0.1$ mm/rev, $a_p = 2$ mm). In 3D FE modelling, constant shear friction factor ($m = 0.9\text{--}0.95$) was used to represent friction between tool and workpiece. The averages, minimum and maximum of the simulated forces (F_c , cutting force, F_t , thrust force and F_z , feed force) are given in Table 3. The simulated cutting forces are found to be in close agreements with the experimental ones as summarized in Table 3.

Predicted temperature distributions (see Fig. 4) depict that the lowest temperature rise in the tool is observed with cBN coated WC/Co tool due to the highest effective thermal conductivity and contact friction. Predicted chip formation is shown in Fig. 5.

3D FE simulations are also utilized to predict tool wear. The tool wear rate models describe the rate of volume loss on the tool rake and flank faces per unit area per unit time. A tool wear rate model based on the adhesive wear proposed by Usui et al. [12] was employed. This model uses interface temperature (T), normal stress (σ_n), and sliding velocity (v_s) at the contact surfaces as inputs and yields tool wear rate (dW/dt) for a given location on the tool surface as shown in Eq. (2). The constants of this equation are set to

$c_1 = 7.8 \times 10^{-9}$ and $c_2 = 2.5 \times 10^3$ in the FE simulations. Determining these constants could be extensive work so they are kept same for simplicity. Chiefly crater wear was observed on all of the tools under these cutting conditions. Fig. 6 shows the comparison of measured and simulated tool wear zones.

$$dW/dt = c_1 \sigma_n v_s \exp\left(\frac{-c_2}{T}\right) \quad (2)$$

5. Conclusions

In this study, a modified material model for Ti-6Al-4V titanium alloy is developed where strain (flow) softening, strain hardening and thermal softening effects are coupled. This model is validated with elasto-viscoplastic FE simulation of adiabatic shearing based serrated chip formation in machining Ti-6Al-4V titanium alloy. The simulation predictions are compared with orthogonal cutting test results by using measured forces and chip morphology. Turning experiments have been conducted with uncoated, mono and multi-layer coated WC/Co carbide tools and cutting performance of these coatings are evaluated. Although cBN and TiAlN + cBN coated WC/CO inserts exhibit largest cutting forces at higher cutting speeds, they reveal favourable wear development. Tool wear zone measurements and predictions show that cBN coated WC/Co inserts depict smallest wear zone. Consequently, cBN coatings may lead to reduction in tool wear dry machining of titanium alloyed Ti-6Al-4V material.

Acknowledgements

The authors gratefully acknowledge the support by the National Science Foundation (CMMI-0758820 and CMMI-0757954), and BOREN Institute of Turkey.

References

- [1] Byrne G, Dornfeld D, Denkena B (2003) Advanced Cutting Technology. *CIRP Annals* 52(2):483–507.
- [2] Cotterell M, Byrne G (2008) Dynamics of Chip Formation during Orthogonal Cutting of Titanium Alloy Ti-6Al-4V. *CIRP Annals* 57:93–96.
- [3] Corduan N, et al, (2003) Wear Mechanisms of New Tool Materials for Ti-6Al-4V High Performance Machining. *CIRP Annals* 52(1):73–76.
- [4] Bouzakis K-D, et al, (2009) Application in Milling of Coated Tools with Rounded Cutting Edges after Film Deposition. *CIRP Annals* 58(1):61–64.
- [5] Komanduri R, von Turkovich BF (1981) New Observations on the Mechanism of Chip Formation When Machining Titanium Alloys. *Wear* 69:179–188.
- [6] Shivpuri R, Hua J, Mittal P, Srivastava AK (2002) Microstructure-Mechanics Interactions in Modelling Chip Segmentation During Titanium Machining. *CIRP Annals* 51(1):71–74.
- [7] Nemat-Nasser S, et al, (2001) Dynamic Response of Conventional and Hot Isostatically Pressed Ti-6Al-4V Alloys: Experiments and Modelling. *Mechanics of Materials* 33:425–439.
- [8] Lee WS, Lin CF (1998) Plastic Deformation and Fracture Behaviour of Ti6Al4V Alloy Loaded with High Strain Rate Under Various Temperatures. *Materials Science and Engineering A* 241:48–59.
- [9] Calamaz M, Coupard D, Girof F (2008) A New Material Model for 2D Numerical Simulation of Serrated Chip Formation When Machining Titanium Alloy. Ti-6Al-4V. *International Journal of Machine Tools and Manufacture* 48:275–288.
- [10] Özel T, Sima M, Srivastava AK (2010) Finite Element Simulation of High Speed Machining Ti-6Al-4V Alloy using Modified Material Models. *Transactions of the NAMRI/SME* 38:1–8.
- [11] Aurich JC, Bil H (2006) 3D Finite Element Modelling of Segmented Chip Formation. *CIRP Annals* 55(1):47–50.
- [12] Usui E, Hirota A, Masuko M (1978) Analytical Prediction of Three Dimensional Cutting Process, Part 3: Cutting Temperature and Crater Wear of Carbide Tool. *Journal of Engineering for Industry* 100:236–243.